



Anodic stripping voltammetry using underpotential deposition allows sub 10 ppb measurement of Total As and As(III) in water

Yifei Zhang, Richard G. Compton^{*}

Department of Chemistry, Physical and Theoretical Chemistry Laboratory, Oxford University, South Parks Road, Oxford, OX1 3QZ, Great Britain, UK

ARTICLE INFO

Keywords:

Underpotential deposition
Anodic stripping voltammetry
Total arsenic detection
As(III)/As(V) speciation
Electroanalysis

ABSTRACT

We report a sensitive stripping voltammetry method for the detection of total arsenic in aqueous solution using gold macroelectrodes based on the underpotential deposition (UPD) of As ad-atoms. The detection of As(III) or total arsenic can be selectively made by changing deposition potential, with detection of the total As content by deposition at high potential (-1.3 V) and of As(III) by deposition at lower potential (-0.9 V). Linear responses were found for both arsenic species in the range $0.01\text{ }\mu\text{M}$ – $0.1\text{ }\mu\text{M}$ at gold macroelectrodes. The analytical useful signals were recorded at concentrations as low as $0.01\text{ }\mu\text{M}$ ($0.8\text{ }\mu\text{g L}^{-1}$) for both arsenic species suggesting that this method can be used to detect total arsenic concentrations in drinking water within the threshold value of the WHO of $0.13\text{ }\mu\text{M}$ ($10\text{ }\mu\text{g L}^{-1}$).

1. Introduction

Anodic stripping voltammetry (ASV) is a widely employed method in electroanalytical chemistry for quantitative measurements of target species in solution, which involves a pre-concentration and a stripping step [1–3]. The pre-concentration step allows the accumulation by electro-reduction of analytes onto the surface of electrode, whilst the stripping step is conducted by scanning the voltammetry anodically, which produces a stripping peak allowing the characterization and quantification of the target [1–3]. In comparison with other direct forms of voltammetry such as cyclic and linear sweep voltammetry, ASV offers lower limits of detection (LODs) (10^{-10} – 10^{-11} M) and higher sensitivities (10^3 A M^{-1}) because the pre-concentration step, which can be applied for as long as is needed, circumvents the limitation imposed by the rate of diffusion of analytes from bulk solution to the surface of electrode [4–6]. The method has been widely used for detection of heavy metal ions in drinking water via the detection of bulk metals for example in respect of arsenic [7–10], copper [11–13], lead [13–15] and mercury [16–18] with low detection limits.

Underpotential deposition (UPD) of a metal onto the surface of electrode in the form of a monolayer or a sub-monolayer takes place at potentials lower than those required for the deposition of the bulk metal [10,19–21]. Our previous proof of concept studies have established the merits of using UPD rather than bulk metal deposition in ASV for As(III) detection, including overcoming the limitations of Cu(II) interference on

both platinum and gold surfaces [7,10], where in particular pre-concentration using UPD prevents a co-deposition of Cu and arsenic and hence interference with the analysis from the widely occurring Cu (II). In the case of Au electrodes it was further shown that chloride ions do not interfere. ASV with UPD was seen to have good sensitivity and, most importantly for application in drinking water, LODs with clear and visually distinct signals within WHO limits [7,10].

Arsenic is the 20th abundant element in natural (0.00005% of the Earth's crust by mass) [22–24]. Arsenic appears in groundwater from both natural sources such as volcanic activity and from human activities such as mining industries [22–24]. There are four recognised oxidation states of arsenic: As(–III), As(0), As(+III) and As(+V). Although many forms of arsenic species have been detected in water samples, the dominant forms of arsenic are arsenite, As(III), and arsenate, As(V) [22, 25,26]. The arsenic species are highly toxic and exposure to arsenic can cause severe health problems including cardiovascular disease and cancer [27–29] and whilst As(III) is thought to be more toxic than As(V) [30], the guidelines for water safety [31] are written in terms of the *total* arsenic content. However most analytical methods for As have focussed on As(III) detection. Rather less attention has been given to As(V) or total arsenic detection [32,33]. In this paper we develop the UPD ASV approach to allow analysis of As(V) and total As in addition to As(III).

Instrumental laboratory based methods have been used for measuring total As including atomic absorption spectrometry (AAS) [34] and inductively coupled plasma mass spectrometry (ICPMS) [35,

^{*} Corresponding author.

E-mail address: Richard.compton@chem.ox.ac.uk (R.G. Compton).

<https://doi.org/10.1016/j.talanta.2022.123578>

Received 1 April 2022; Received in revised form 15 May 2022; Accepted 18 May 2022

Available online 21 May 2022

0039-9140/© 2022 The Authors. Published by Elsevier B.V. This is an open access article under the CC BY license (<http://creativecommons.org/licenses/by/4.0/>).

[36], which provide low detection limits and high sensitivities but require strict sample preparation conditions and special laboratory conditions. Accordingly, we see clear benefits for an electrochemical approach but note that previous electrochemical methods for As(V) show rather high LODs as benchmarked against the WHO safety thresholds. As(V) is typically quantified either by indirectly measuring As(III) formed by chemical reduction of As(V), or directly measured using selective deposition. Sakira et al. used nanogold modified carbon paste electrode for total arsenic contents detection, in which As(V) was chemically reduced to As(III) before analysis [37]. Svancara et al. detected concentrations of As(III) and As(V) using ASV with bulk deposition coupled with homogeneous chemical reduction of the As(V) [38]. The direct electrochemical measurement of As(V) was realised by Postek who used adsorptive stripping voltammetry but could only realise a LOD of 350 ppb [39] which is greatly in excess of the WHO threshold of $10 \mu\text{g L}^{-1}$. Lower LODs were achieved by electrode modification primarily to enhance the active interfacial areas. Thus Zakharova et al. [39] used ASV with bulk deposition to detect As(V) at an Au microwire electrode modified with Mn particles in aqueous 0.1 M Na_2SO_3 with a theoretical LOD of $0.35 \mu\text{g L}^{-1}$ estimated using the 3σ method [40,41]; Huang et al. modified a Pt wire electrode with a Au film and reported a LOD of $0.5 \mu\text{g L}^{-1}$ for As(V) using ASV with bulk deposition with the LOD again calculated with the 3σ method [41,42]; Yamada et al. utilised Au nanoparticles deposited onto boron doped diamond electrode (BDDE) giving a LOD of $100 \mu\text{g L}^{-1}$ for As(V) [43] based on a visually discernible signal. In these methods the use of bulk As deposition in the pre-concentration step makes them inevitably susceptible to interference from Cu [40,42].

In this paper we suggest that the combination of UPD and ASV can solve the problems both of attaining low LODs whilst avoiding the interference from Cu seen when bulk deposition is used. In particular the use of highly negative deposition potentials with longer deposition time for bulk deposition may enhance the sensitivity of the detection method [44] but not the selectivity. UPD, on the other hand, can avoid the formation of alloy or/and the intermetallic species of Cu and As in the pre-concentration step [7,10] since typically sub-monolayer layers are deposited in the preconcentration step. In previous papers, the ASV methods were focused more on the stripping peak of bulk As to obtain low LODs for As(III) [45–47], while in this method, the stripping peak of As ad-atoms due to UPD was explored for the observation of low detection limits. In the following we apply UPD-ASV with deposition on a gold electrode at a potential where both As(V) and As(III) are deposited in sub monolayer amounts to give the total arsenic concentrations in water. This is then followed by measurements of UPD-ASV at a potential where As(III) is selectively deposited, but not A(V) [10]. The concentrations of As(V) then can be determined by subtraction from the total arsenic concentration of the As(III) concentration. The LOD is determined from analytically useful signals in the sub $10 \mu\text{g L}^{-1}$ range at Au macroelectrodes. In this way the As(III), As(V) and total As content of aqueous solutions are found for levels of As at and below the WHO recommended level of $10 \mu\text{g L}^{-1}$ for drinking water.

2. Experimental

2.1. Chemical reagents

Commercially available sodium hydrogen arsenate heptahydrate (Na_2HAsO_4 , 98%, Alfa Aesar, UK), sodium (meta) arsenite (NaAsO_2 , 99%, Fluka, Switzerland), and sulphuric acid (H_2SO_4 , 98%, Fisher Scientific, UK) were purchased and used without any further purification. All aqueous solutions were prepared using deionized water (Milipore, UK) with a resistivity of $18.2 \text{ M}\Omega \text{ cm}$ at 298 K.

2.2. Instrumentation

All electrochemical measurements were conducted with a standard

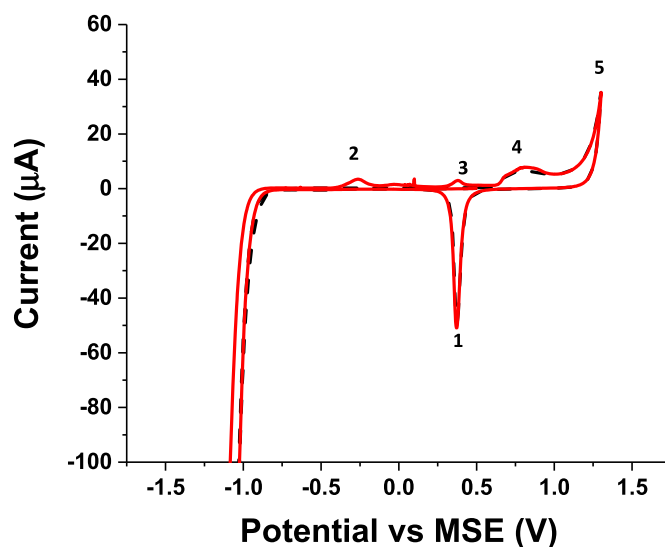


Fig. 1. CV of 500 μM As(V) in 0.1 M H_2SO_4 (red) and blank solution (black dashed line) at Au macroelectrodes. The voltammograms were conducted from $+0.5 \text{ V}$ vs MSE and first scanned cathodically to -1.4 V at a scan rate of 0.1 V s^{-1} followed by an anodic scan to $+1.3 \text{ V}$. (For interpretation of the references to colour in this figure legend, the reader is referred to the Web version of this article.)

three-electrode system in a Faraday cage and were thermostatted at 298 (± 0.1) K. A carbon rod served as a counter electrode and a mercury-mercurous sulfate electrode (MSE, BASi, USA) served as the reference electrode with a potential of $+0.65 \text{ V}$ vs. standard hydrogen electrode (SHE) [48], and the solution used in the reference electrode was aqueous saturated K_2SO_4 (1.45 M). A gold macroelectrode (diameter of $1.60 \pm 0.01 \text{ mm}$, geometric area of 0.02 cm^2 , BASi, USA) or a gold screen printed electrode (Au SPE) operated as a working electrode. The Au SPEs were purchased from Drop Sens (DS, geometric area of 0.13 cm^2 , Spain), Zensor (Zen, geometric area of 0.2 cm^2 , TW) and Zimmer & Peacock (ZP, geometric area of 0.04 cm^2 , Norway). All Au SPEs were used without further modifications. The surfaces of Au SPEs from ZP were cleaned with 10 mM HCl before electrochemical measurements based on a method recommended by the supplier [49]. The Au SPEs from the other two companies were used without pre-cleaning. The Au macroelectrode was polished with alumina before each measurement. All electrochemical measurements were performed in 0.1 M H_2SO_4 with various concentrations of arsenic, and were recorded with a $\mu\text{Autolab}$ type III potentiostat (EcoChemie, NL) after degassing with nitrogen.

3. Results and discussion

In this section, first, the electrochemical behaviour of As(V) is studied in 500 μM Na_2HAsO_4 in 0.1 M H_2SO_4 with the latter present to control the pH and act as supporting electrolyte. Cyclic voltammetry (CV) and anodic stripping voltammetry (ASV) are the electrochemical techniques used. The peaks in the CVs are assigned, and the presence of a UPD peak is noted in the ASV. Then the method of anodic stripping voltammetry with underpotential deposition (UPD) previously reported for As(III) is then extended and, for the first time, applied to the measurement of As(V) and total As concentrations realising a low detection limit, as assessed on the basis of visually clear signals, for As(V) of $0.8 \mu\text{g L}^{-1}$ well within the WHO limit of $10 \mu\text{g L}^{-1}$ for safe drinking water. Finally, the determination of the total arsenic concentration and of the individual concentrations of As(III) and As(V) in mixtures of As(III) and As(V) is established using the UPD-ASV method.

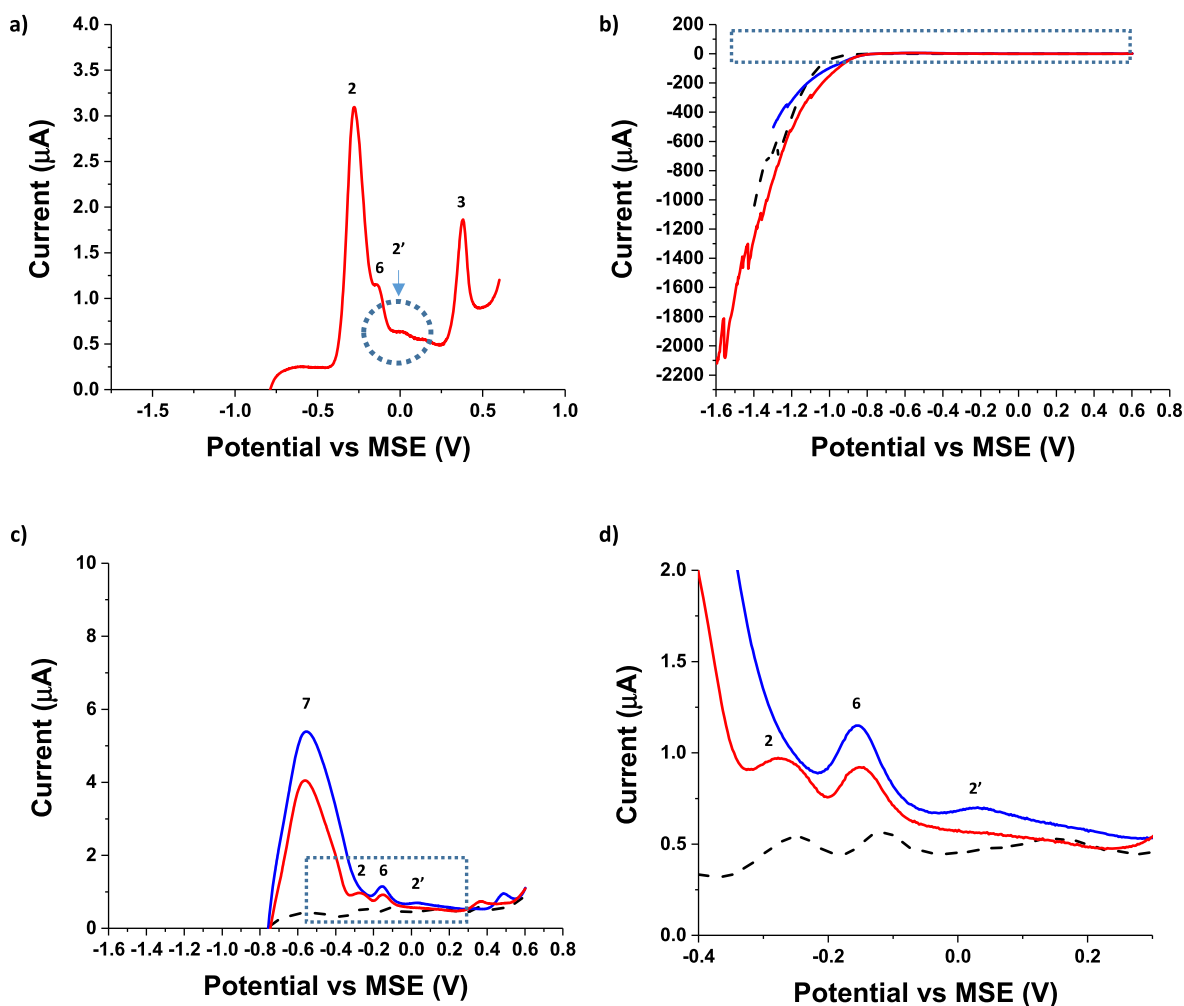


Fig. 2. a) Anodic stripping voltammograms of 10 μM As(V) in 0.1 M H_2SO_4 at a gold macroelectrode with a pre-concentration at -1.3 V for 300 s. b) Anodic stripping voltammograms of 0.1 M H_2SO_4 (black dashed line), 0.1 μM As(V) in 0.1 M H_2SO_4 with deposition at -1.6 V for 300 s (red) and -1.3 V for 300 s (blue). c) is the magnification of framed part in b). d) is the magnification of framed part in c). In b), c) and d), the lines represent the voltammograms of 0.1 M H_2SO_4 (black dashed line), 0.1 μM As(V) in 0.1 M H_2SO_4 with deposition at -1.6 V for 300 s (red) and -1.3 V for 300 s (blue) at a scan rate of 0.1 V s^{-1} . (For interpretation of the references to colour in this figure legend, the reader is referred to the Web version of this article.)

3.1. Electrochemical response of As(V) on Au electrodes

3.1.1. Cyclic voltammetry of As(V)

To facilitate electrochemical analysis of As(V), cyclic voltammetry and anodic stripping voltammetry were first conducted at a gold macroelectrode. The pH of the electrolyte was 1, which kept the arsenic species into their acid forms as arsenic acid (H_3AsO_4) for As(V) and arsenious acid (H_3AsO_3) for As(III) since their pK_a are 2.19 and 9.2 respectively [50]. Fig. 1 illustrates the CV response of 500 μM Na_2HAsO_4 in 0.1 M H_2SO_4 with a potential window from -1.4 V to $+1.3$ V (vs. MSE) at a gold macroelectrode. The voltammograms shown are the first scans made after polishing the electrode with alumina. The CV was started at $+0.5$ V and first scanned cathodically to -1.4 V, then scanned anodically to $+1.3$ V at a scan rate of 0.1 V s^{-1} . Two features are observed on the forward. Peak 1 observed at $+0.37$ V is assigned to the reduction of Au oxide to Au [51,52]. Solvent decomposition onsets at potentials around -1.3 V and comprises a mixture of the hydrogen evolution reaction (HER) [51] and the reduction of As(V) to bulk As(0) [42]. On the reverse anodic scan, four peaks were observed, denoted as peaks 2, 3, 4 and 5. Peak 2 with the potential of ca -0.3 V represents the oxidation of bulk As(0) to As(III) [10,52]. The peak 3 observed at $+0.4$ V corresponds to the oxidation of As(III) to As(V) [10,40]. Peak 4 at $+0.8$ V was ascribed to the oxidation of Au to Au oxide [51], and peak

5 at ca $+1.3$ V was considered to be the start of oxygen evolution reaction (OER) [52]. Comparing with the voltammogram that obtained in blank solution (0.1 M H_2SO_4 , black dashed line in Fig. 1), two peaks were absent in blank solution (peaks 2 and 3) which all relate to arsenic, whilst peaks 1, 4 and 5 were ascribed to the reduction of Au oxide, oxidation of Au and OER, respectively [52].

3.1.2. Deposition and stripping of As

To further understand the electrochemistry of As(V) on the surface of gold electrodes, a 10 μM solution of Na_2HAsO_4 in 0.1 M H_2SO_4 was examined via ASV (Fig. 2a). Pre-concentration was conducted at -1.3 V for a period of 300 s to electro-reduce the As(V) to deposit As in the form of both bulk As and UPD As after which the potential was swept from -1.3 V to $+0.6$ V at a scan rate of 0.1 V s^{-1} . In Fig. 2a, four peaks were observed labelled as 2, 2', 3 and 6. Peaks 2 and 3 represent the same chemistry shown above. Peak 6 observed at ca -0.15 V is related to the deposition of H atoms and the deposition potential [8,51]. The peak 2' at ca $+0.04$ V was assigned as the stripping peak associated with the oxidation of As(0) ad-atoms to As(III) [10,53,54].

To understand the relationship between the bulk As (peak 2) and UPD As (peak 2'), As(V) with much lower concentrations were next studied. A 0.1 μM solution of Na_2HAsO_4 in 0.1 M H_2SO_4 was examined via ASV (Fig. 2b, c and 2d). Pre-concentration was conducted at various

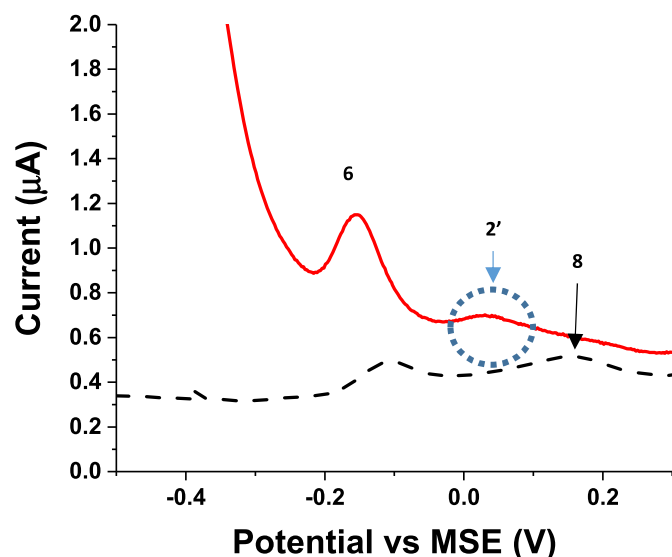


Fig. 3. Magnified anodic stripping voltammograms of 0.1 M H_2SO_4 (black dashed line) and 0.1 μM As(V) with 0.05 μM As(III) in 0.1 M H_2SO_4 (red) at a gold macroelectrode with a pre-concentration at -1.3 V for 300 s. ASV parameters: deposition at -1.3 V for 300 s, potential scan rate 0.1 V s^{-1} . (For interpretation of the references to colour in this figure legend, the reader is referred to the Web version of this article.)

potentials in the range from -1.6 V to -1.3 V for 300 s to reduce the As(V) to deposit As(0) either in the form of bulk As or UPD As after which the potential was swept from the deposition potential to $+0.6$ V at a scan rate of 0.1 V s^{-1} . Fig. 2b illustrates as measured voltammetry of a blank solution (0.1 M H_2SO_4 , black dashed line), and 0.1 μM As(V) in 0.1 M H_2SO_4 with the deposition potentials of either -1.6 V (red) or -1.3 V (blue). The huge reductive currents with the sweep of the potential from -1.6 V to ca -1.0 V is due to the large negative potential leading to the formation of hydrogen during the pre-concentration step. At less negative potentials some of the formed hydrogen is re-oxidised resulting in a peak (labelled peak 7) as seen in Fig. 2c with a peak potential of -0.6 V (Hydrogen oxidation reaction, HOR) [51]. The part of the voltammogram showing positive currents was magnified (framed area of Fig. 2b) and is shown in Fig. 2c. Peaks 2, 2' and 6 represent the chemistry discussed above. To further discuss the peaks of bulk As, peak 2 and UPD As, peak 2', the framed area of the voltammogram is further magnified and is shown in Fig. 2d.

Fig. 2d illustrates the ASV response of 0.1 μM Na_2HAsO_4 in 0.1 M H_2SO_4 with deposition at -1.6 V for a period of 300 s (red) and that with deposition at -1.3 V for 300 s (blue). Three peaks can be observed, labelled as 2, 2' and 6, where they all represent the chemistry inferred above. It is apparent that bulk As is deposited at potentials more negative than -1.4 V, whereas UPD As is essentially exclusively deposited at the less negative potential of -1.4 V at the concentration of As(V) and the deposition times studied (red line in Fig. 2d). Deposition at more negative potentials than -1.3 V likely causes increased evolution of H_2 gas, which may affect the reproducibility of the stripping analysis [43, 51] in addition to the formation of bulk As(0). The potential of -1.3 V was selected as enabling the formation of As ad atoms whilst minimising the possible formation of hydrogen bubbles and avoiding the deposition of bulk As (blue line in Fig. 2d).

3.2. The analytical use of as UPD signals

The UPD-ASV method for the detection of low concentrations of As(III) on gold was introduced via proof-of-concept by the present authors to eliminate the problems of interferences when bulk solids are deposited as the pre-concentration for ASV [10]. In this paper, UPD-ASV is

first applied for the detection of the total As content (As(V) + As(III)), then selectively detect the concentration of As(III) in mixtures with As(V) in water using gold macroelectrodes. Subtraction of the two results then allows estimates of the As(V) content. For As(V) detection in solutions containing only As(V) or for the measurement of the total As concentrations in mixtures of As(III) and As(V), the pre-concentration of As(0) was first carried out at -1.3 V for a period of 300 s, which results in As ad-atoms being deposited at the surface of gold [40,42,43]. Note that at high concentrations of As(V) or for more prolonged deposition, as reported and quantified below, bulk As is deposited likely physically on the top of the layer of ad-atoms so the procedure is specific for the measurement of As at low concentrations appropriate for the detection of As in drinking water, the usual reason for detecting As. Following pre-concentration a linear sweep scan was applied from -1.3 V to $+0.6$ V at a scan rate of 0.1 V s^{-1} to strip the As ad-atoms. The charge of the stripping peak was used as the signal to quantify the concentration of As(V) in solutions of only As(V) or the total concentration for As in dilute mixtures. Fig. 3 shows the magnified ASV of 0.1 μM As(V) with 0.05 μM As(III) in 0.1 M H_2SO_4 . Two peaks can be observed, peaks 2' and 6, which were ascribed to the chemistry discussed above. The peak of bulk As, peak at ca -0.3 V cannot be observed, which means there is no bulk As deposited for As(III) at this concentration of mixture of arsenic. Note that in the blank solution (black dashed line in Fig. 3), two small peaks can be observed, peaks 6 and 8, where peak 6 reflects chemistry shown above and peak 8 at ca $+0.15$ V represents an oxidation of gold at the surface of electrode [53].

For As(III) detection, both in solutions containing only As(III) and in mixtures with As(V), the pre-concentration was carried out at -0.9 V for 300 s then followed with a linear sweep voltammetry (LSV) from -0.9 V to $+0.6$ V at a scan rate of 0.1 V s^{-1} , and the charge of the stripping peak was used for the quantification of As(III). Baseline correction was applied to the voltammograms (see Supporting Information (SI) Section 1 for procedure), then the charge of the stripping peak was calculated from the peak area of baseline corrected voltammogram (shown in SI Section 2).

3.2.1. Observations of As(V) and As(III) UPD stripping signals

To examine the capability of the UPD-ASV method for arsenic detection in water, experiments were first conducted in various concentrations of As(V) in 0.1 M H_2SO_4 using Au macroelectrodes. The pre-concentration of As(0) was first carried out at -1.3 V for 300 s in various concentrations of As(V) then followed with a linear potential sweep from -1.3 V to $+0.6$ V at a scan rate of 0.1 V s^{-1} . Fig. 4a illustrates the baseline corrected linear sweep voltammetric responses of peak 2' at gold macroelectrodes measured in As(V) solutions of concentration ranging from $0.01 \mu\text{M}$ to $1 \mu\text{M}$ in 0.1 M H_2SO_4 . The stripping peak was observed at ca $+0.04$ V and the charge of the peak increased with the concentration of As(V). Fig. 4c shows the plot of charges of peak 2' against concentrations of As(V) (red). The charges first increased linearly and rapidly but then increasingly slowly until a plateau was attained at ca $1 \mu\text{M}$ consistent with the formation of 0.007 layers of As ad-atoms (See SI Section 3 for calculations). This is as expected for the formation of a UPD layer. The $1 \mu\text{M}$ As(V) corresponds to a surface coverage of ca $(5 \pm 0.2) \times 10^{12} \text{ molecules cm}^{-2}$ and ca 0.007 monolayers. It sets an upper limit (ca $1 \mu\text{M}$, $75 \mu\text{g L}^{-1}$) for detection of As(V) via UPD-ASV method using the charge of stripping peak at Au macroelectrodes and provide a visually clear signal for concentrations as low as $0.01 \mu\text{M}$ ($0.8 \mu\text{g L}^{-1}$, See SI section 1 for baseline correction method). The range thus spans that likely to be encountered in drinking water with a limit of $10 \mu\text{g L}^{-1}$ [31].

Analogous experiments were also made for As(III) detection as follows; the pre-concentration of As ad-atoms was carried out at -0.9 V for 300 s in various concentrations of As(III) solution then a linear potential scan was made at a scan rate of 0.1 V s^{-1} . The baseline corrected LSVs are shown in Fig. 4b, in which can be seen that the charge of the peak increased with the concentrations of As(III). The charges of stripping

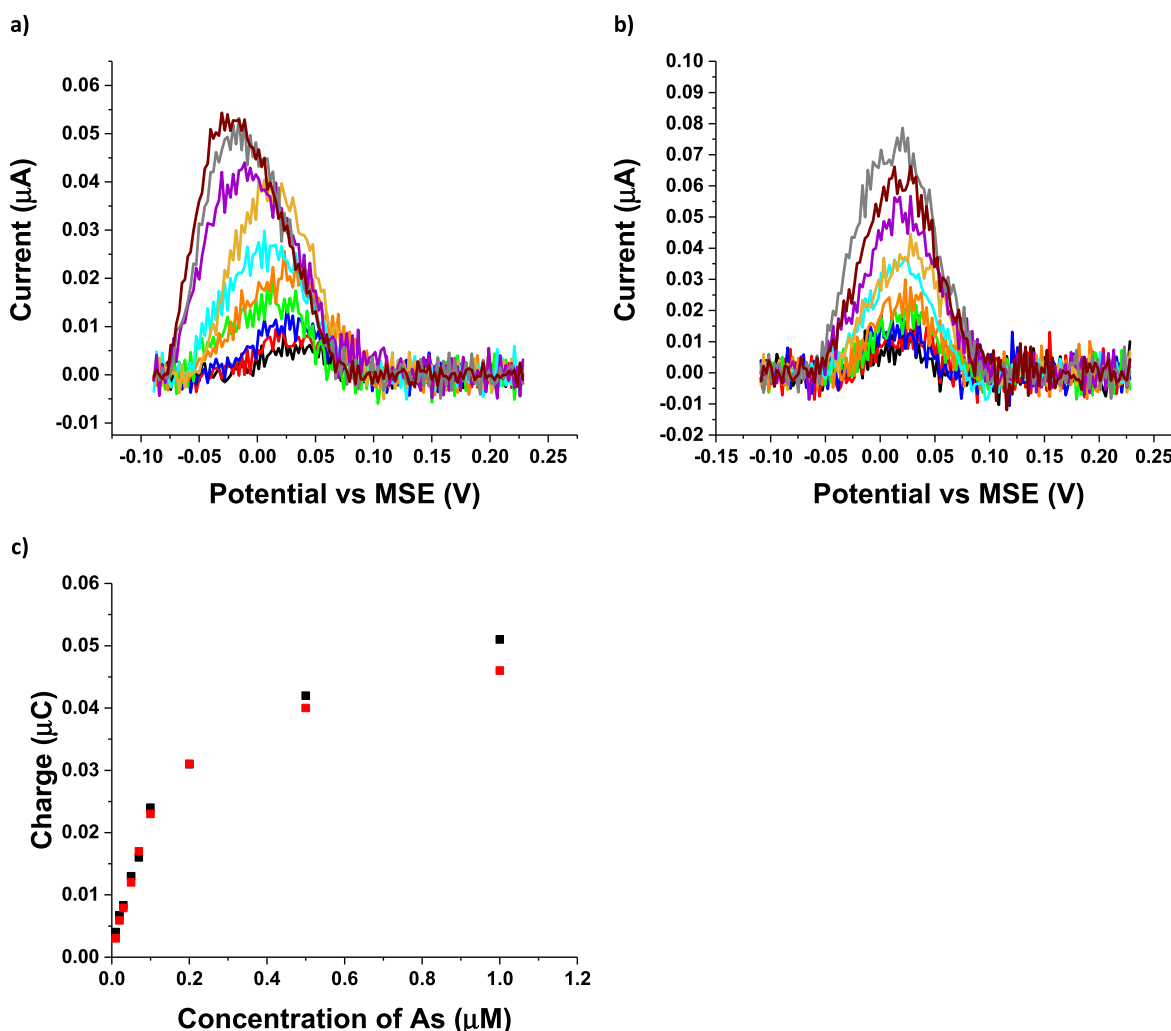


Fig. 4. Baseline corrected stripping voltammograms of various concentrations of a) As(V) or b) As(III) in 0.1 M H₂SO₄ at Au macroelectrodes. c) Also shown are plots of the charge of peak 2' vs concentrations of As(V) (red) or As(III) (black), in 0.1 M H₂SO₄ at Au macroelectrodes. The concentrations of As(V) were 0.01 μM (black), 0.02 μM (red), 0.03 μM (blue), 0.05 μM (green), 0.07 μM (orange), 0.1 μM (cyan), 0.15 μM (yellow), 0.2 μM (purple), 0.5 μM (grey), and 1 μM (brown). ASV parameters: deposition at -1.3 V vs. MSE for 300 s, potential scan rate 0.1 V s⁻¹, and baseline was modelled via polynomial method from -0.1 V to +0.22 V for peak 2'. (For interpretation of the references to colour in this figure legend, the reader is referred to the Web version of this article.)

peaks plotted against the concentration of As(III) are shown in Fig. 4c (black). A similar phenomenon can be seen as observed for As(V) with similar limiting coverages (ca 0.007 ML) in the range 0–1 μM (See SI Section 3 for calculation). In the case of concentrations above 1 μM As(III) shows slightly higher coverages than seen for As(V) which may reflect the onset of for further UPD deposition on different sites to those occupied at lower coverages. However the bespoke analytical procedure is designed for low concentrations well below 1 μM.

The analytical measurements in this study were then based on the sub-monolayer of deposited As(0) ad-atoms from As(III), As(V) or both arsenic species. Although the charge of stripping peak increased with the concentrations of arsenic in the range from 0.01 μM to 1 μM with similar sensitivities for As(III) and As(V), it is preferable to find a linear relationship so that the sensitivity can be calculated. Further attention was thus focused on the use of UPD-ASV at lower concentrations of arsenic species.

3.2.2. Calibration curves, sensitivities and limits of detection

To determine the sensitivities of As(III) and As(V) under analysis via UPD-ASV, and to identify linear ranges and detection limits, concentrations of As(III) and As(V) below 0.1 μM were studied on gold macroelectrodes. The upper limit was defined by the WHO drinking water

limits [31]. The linear range and sensitivity was investigated for As(V) first. To measure the concentrations of As(V) in 0.1 M H₂SO₄, pre-concentration was carried out at -1.3 V for 300 s then followed up with a linear potential sweep from -1.3 V to +0.6 V at a scan rate of 0.1 V s⁻¹. Baseline corrections were applied as above. Fig. 5a illustrates the baseline corrected stripping voltammograms of peak 2' for analyte concentrations in the range of 0.01 μM–0.1 μM As(V) at Au macroelectrodes. The peak 2' was observed at ca +0.04 V and the charge of the stripping peak increased with the concentrations. To obtain the relationship between the charge of peak 2' and the concentration of As(III) at Au macroelectrodes, the charges of stripping peak were plotted against the concentrations in Fig. 5b. A linear relationship, $Charge = 2.2 \times 10^{-7} C \mu M^{-1} \times [As(V)] + 7 \times 10^{-10} C$, was inferred over the range of concentrations studied. The error bars shown are standard deviations calculated from at least three sets of data. Rather than calculating the LOD using the 3σ method [41], which may not give a realistically low detection limit since σ can be small and result in an extremely low and artificial LOD [41], we used the 'practical detection limits' based on the concentration giving visually clear signals [7,10], and identified the LOD to be 0.01 μM (0.8 μg L⁻¹) with the sensitivity of $2.2 \times 10^{-7} C \mu M^{-1}$ for As(V) at the Au macroelectrodes.

Fig. 5c illustrates the raw voltammogram (black line in Fig. 5c) in the

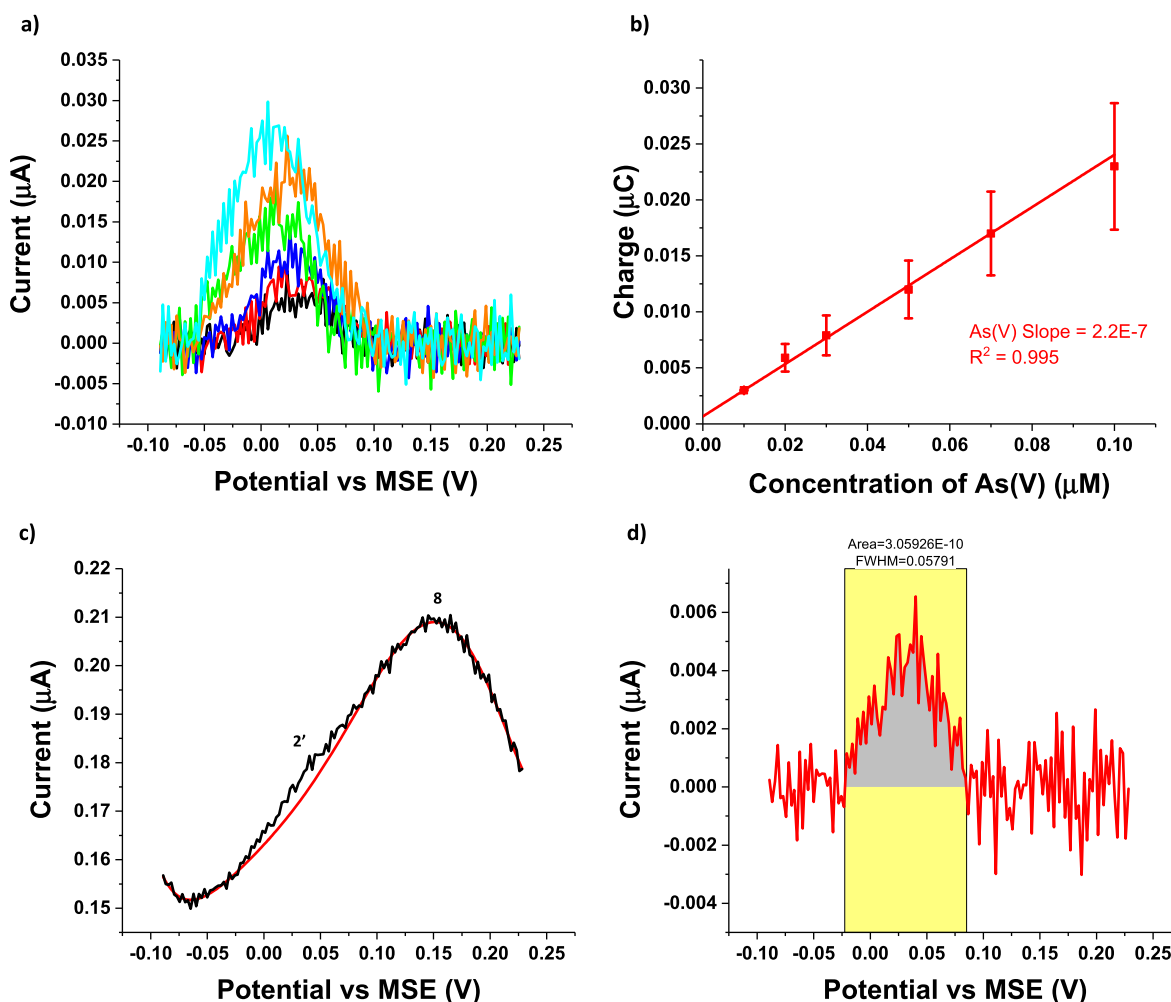


Fig. 5. a) Baseline corrected stripping voltammograms of various concentrations of As(V) in 0.1 M H_2SO_4 at Au macroelectrodes. Also shown are plots of the charge of peak 2' vs concentrations of b) As(V) in 0.1 M H_2SO_4 at Au macroelectrodes. The concentrations of As(V) were 0.01 μM (black), 0.02 μM (red), 0.03 μM (blue), 0.05 μM (green), 0.07 μM (orange), and 0.1 μM (cyan). The charge was calculated from baseline corrected LSVs and the error bars shown are standard deviations calculated from at least three sets of data. c) The unmodified LSV curve from -0.10 V to $+0.22$ V (black line) and simulated baseline (red line). d) The baseline corrected LSV curve from -0.10 V to $+0.22$ V (red line) and the peak area (grey area). ASV parameters: deposition at -1.3 V vs. MSE for 300 s, potential scan rate 0.1 V s^{-1} , and baseline was modelled via the polynomial method from -0.1 V to $+0.22$ V for peak 2'. (For interpretation of the references to colour in this figure legend, the reader is referred to the Web version of this article.)

potential range of -0.1 V to $+0.22$ V. The peak 2' at ca $+0.04$ V was a shoulder of the bigger peak (peak 8) that reflects the oxidation of gold on the surface electrode as above [53] when the concentration of As(V) was as low as 0.01 μM . The peak current of peak 2' increased with the concentrations of arsenic and reached a similar height as peak 8 when the concentration was 0.1 μM . When the concentration of arsenic was higher than 0.1 μM , the peak current of peak 2' became higher than that of peak 8. Thus a baseline correction was required to eliminate the influence from the background signal. A baseline (red line in Fig. 5c) was simulated via the polynomial method in Origin 2017 with an order of 7 from -0.08 V to -0.05 V and $+0.095$ V to $+0.22$ V. Thus, the simulated background line in the Fig. 5c was in the range from -0.05 V to $+0.095$ V. To calculate the charge of the stripping peak of UPD As, a subtraction between the unmodified voltammogram and the simulated baseline was applied, and the baseline corrected voltammogram is shown in Fig. 5d. The area of peak 2' (grey area in Fig. 5d) can be calculated via 'integrate' in Origin and the charge of the peak then can be determined (See details in SI Section 2). These parameters were used for the whole project for baseline corrections of peak 2'. To further explore the practical use of this method on arsenic species detection, analogous experiments were made for As(III) at Au macroelectrodes for comparison with that for As(V).

Pre-concentration of As(0) from As(III) was carried out at -0.9 V for 300 s in various concentrations of As(III) solution then a linear potential sweep was made from -0.9 V to $+0.6$ V at a scan rate of 0.1 V s^{-1} at Au macroelectrodes. Baseline correction followed the procedure above. Fig. 6a presents the baseline corrected voltammograms of As(III) at Au macroelectrodes that were measured for concentrations in the range from 0.01 μM to 0.1 μM . The peak 2' was observed at ca $+0.04$ V and the charge increased with the concentrations of As(III). Then the charge of peak 2' was plotted against the concentrations of As(III) in Fig. 6b. The linear relationship, $\text{Charge} = 2.1 \times 10^{-7} \text{ C } \mu\text{M}^{-1} \times [\text{As(III)}] + 2 \times 10^{-9} \text{ C}$, was obtained in the range of 0.01 μM – 0.1 μM , and the error bars were again calculated from at least three sets of data. The LOD was inferred from analytical useful signals rather than the 3σ method, and was determined to be 0.01 μM (0.8 $\mu\text{g L}^{-1}$), and the sensitivity was $2.1 \times 10^{-7} \text{ C } \mu\text{M}^{-1}$ for As(III). In comparison with the results of As(V), both arsenic species had the same LOD, 0.8 $\mu\text{g L}^{-1}$, and a similar sensitivity, $2.1 \times 10^{-7} \text{ C } \mu\text{M}^{-1}$. The detection limit, 0.8 $\mu\text{g L}^{-1}$ obtained using analytically clear signals meets, by a considerable margin the WHO guidelines for arsenic in drinking water (10 $\mu\text{g L}^{-1}$) [31]. The similar sensitivity, $2.1 \times 10^{-7} \text{ C } \mu\text{M}^{-1}$ proves that the signal of UPD As increased in a comparable manner with concentration for both As(III) and As(V).

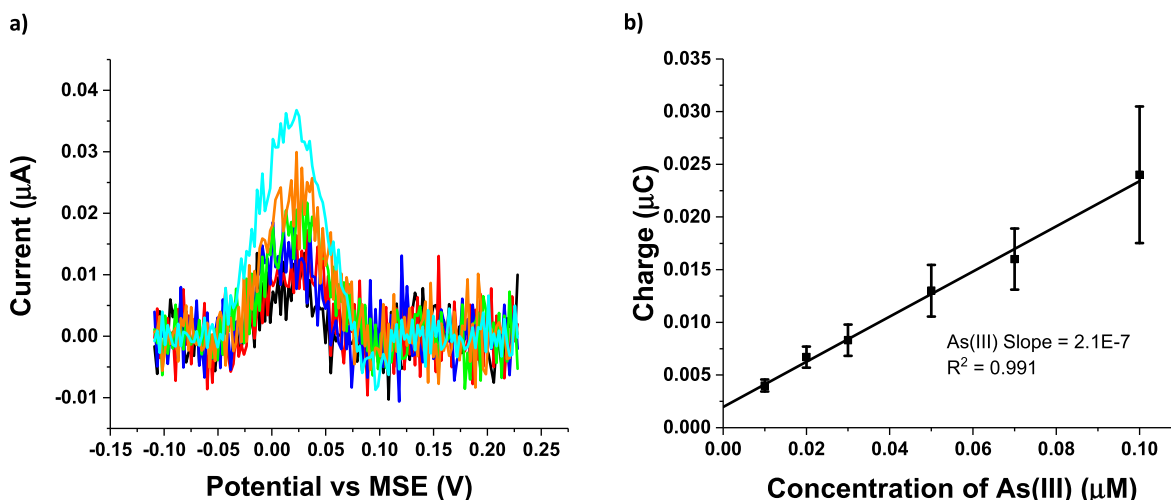


Fig. 6. a) Baseline corrected stripping voltammograms of various concentrations of As(III) in 0.1 M H₂SO₄ at Au macroelectrodes. Also shown are plots of the charge of peak 2' vs concentrations of b) As(III) in 0.1 M H₂SO₄ at Au macroelectrodes. The concentrations of As(III) were 0.01 μM (black), 0.02 μM (red), 0.03 μM (blue), 0.05 μM (green), 0.07 μM (orange), and 0.1 μM (cyan). The charge was calculated from baseline corrected LSVs and the error bars shown are standard deviations calculated from at least three sets of data. ASV parameters: deposition at - 0.9 V vs. MSE for 300 s, potential scan rate 0.1 V s⁻¹, and baseline was modelled via the polynomial method from - 0.1 V to +0.22 V for peak 2'. (For interpretation of the references to colour in this figure legend, the reader is referred to the Web version of this article.)

This observation allows us to use deposition at - 1.3 V to deposit As ad-atoms simultaneously from solution of As(III) or As(V) at the same rate for each species. Accordingly, we were able to apply the method to mixtures of the two species so as to permit the detection of total As concentrations. In the following section these measurements are explored and then combined with deposition at - 0.9 V to give the As(III) content, hence allowing by difference the measurement of the As(V) content.

3.3. Detection of the total as concentration and the As(V)/As(III) speciation

Having tested the capability of the UPD As peak for the detection of As(III) and As(V) separately at gold macroelectrodes, further experiments were conducted to explore if this method can detect both the total amount of arsenic species as well as As(III) and As(V) individually with obvious benefits for application in the real world. Thus, in this section, first various concentrations of As(III) in the presence of different levels of As(V) were analysed for the determination of As(III) using a deposition potential of - 0.9 V. Then a range of concentrations of As(V) in the presence of different amounts of As(III) were analysed for the total concentrations of arsenic using a deposition potential of - 1.3 V. The As(V) concentrations were obtained by subtraction of the As(III) concentration from the total arsenic concentration.

3.3.1. Detection of As(III) in the presence of As(V) in solution

Concentrations of As(III) in the presence of As(V) in 0.1 M H₂SO₄ were measured first, in which a pre-concentration was conducted at - 0.9 V for 300 s then followed with a linear potential sweep from - 0.9 V to + 0.6 V at a scan rate of 0.1 V s⁻¹. Fig. 7a, b and 7c show the baseline corrected voltammograms of As(III) in the presence of 0.1 μM As(V), 0.5 μM As(V) and 5 μM As(V), respectively. From all these three voltammograms, the peak charges of peak 2' increased with the concentrations of As(III) and the charges were similar no matter the concentrations of As(V) were present in the solution. To further understand whether or not the As(V) interfere with the signal of As(III), the peak charges of peak 2' were plotted against the concentrations of arsenic in Fig. 7d. It is clear to see that the sensitivities were similar. The sensitivity of As(III) in the absence of As(V) was $(2.1 \pm 0.2) \times 10^{-7} \text{ C } \mu\text{M}^{-1}$ whilst the sensitivities in the presence of As(V) were ca $(2.0 \pm 0.3) \times 10^{-7} \text{ C } \mu\text{M}^{-1}$, which is

similar. The presence of As(V) did not interfere with the signals of As(III). In addition, the method of using UPD As can be used for the selective detection of As(III) in the presence of As(V) using deposition at - 0.9 V. To further test the capability of detecting total arsenic concentrations by tuning deposition potentials, analogous experiments were made in various concentrations of As(V) in the presence of As(III) with a deposition potential of - 1.3 V.

3.3.2. Detection of As(V) in the presence of As(III) in aqueous solution and the measurement of total arsenic concentrations

Total arsenic concentrations were then measured in mixtures of As(III) and As(V) over a total As concentration range of 0.11 μM (8.25 μg L⁻¹) to 0.35 μM (26.25 μg L⁻¹). Pre-concentration was conducted at - 1.3 V for 300 s then a linear potential scan was made from - 1.3 V to +0.6 V at a scan rate of 0.1 V s⁻¹. Table 1 (Columns 1 and 4) shows the concentrations of As(III) and As(V) in the mixture, and the concentrations determined using UPD-ASV. The latter were based on the charges that obtained from the peak 2' (See calculations in SI Section4). The measured total arsenic concentrations were within the range of ca 10% of the known total arsenic concentrations, signalling that the UPD-ASV method can be used for the detection of total arsenic concentrations in drinking water using a deposition potential of - 1.3 V noting that the key deliverable of the analysis is that the total As concentration lies below the WHO threshold of 10 μg L⁻¹ (0.13 μM) [31].

Next, the As(III) content of the mixtures were found. Pre-concentration was applied at - 0.9 V for 300 s and then followed with a linear potential sweep from - 0.9 V to +0.6 V at a scan rate of 0.1 V s⁻¹. Table 1 (Columns 2 and 5) presents the concentrations of the known As(III) in solution and the measured As(III) concentrations. It shows that the measured As(III) concentrations were within 10% of the known values confirming that the UPD-ASV method can be applied onto determination of As(III) in the mixture of both arsenic species using the deposition potential of - 0.9 V. The standard deviations were estimated from at least of three sets of data from the charge of the stripping peaks of As ad-atoms. Then the concentration was estimated with the equation, $\text{Charge} = 2.2 \times 10^{-7} \text{ C } \mu\text{M}^{-1} \times [\text{As}] + 7 \times 10^{-10} \text{ C}$ and the error was accumulated from the calculation (See sample calculations in SI Section 4).

Finally, the concentrations of As(V) were calculated by subtraction of the measured As(III) concentrations from the measured total arsenic

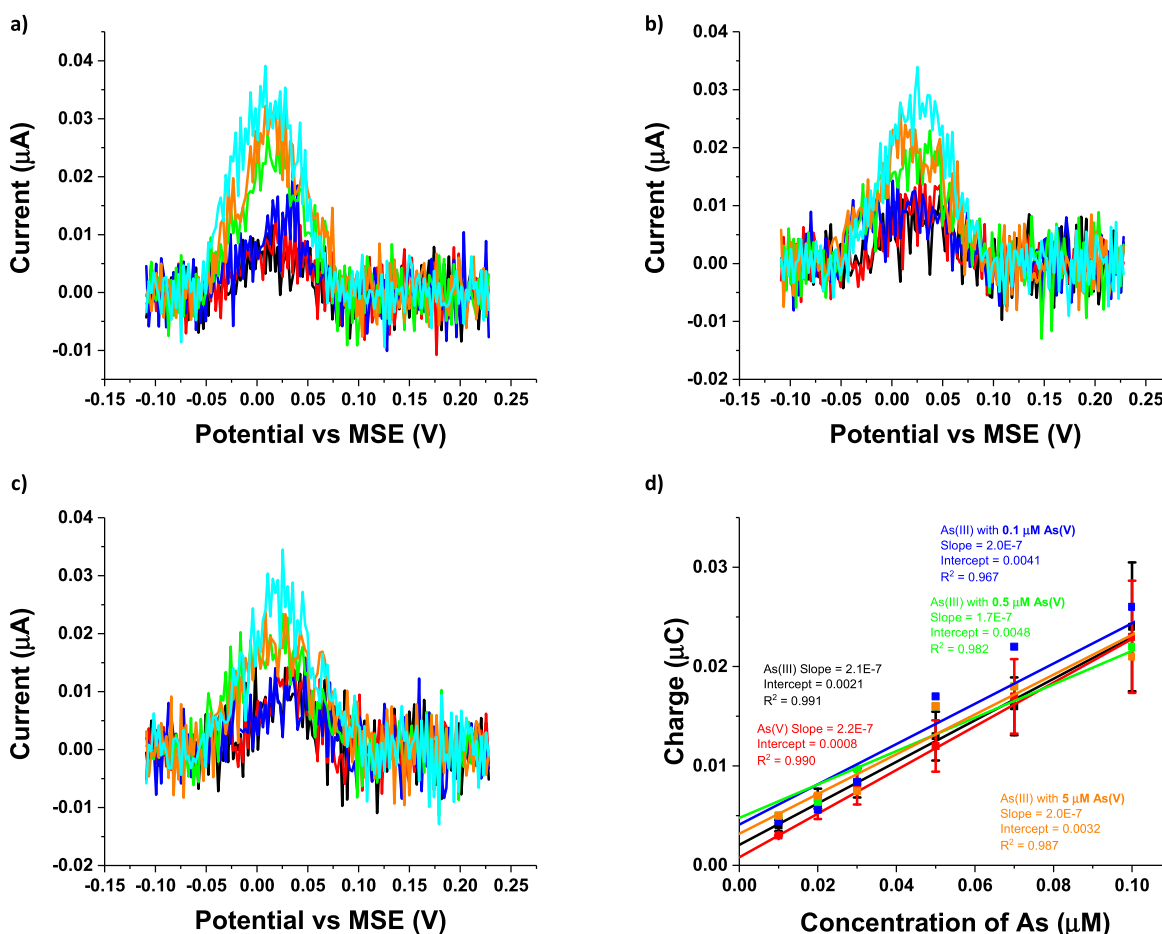


Fig. 7. Baseline corrected stripping voltammograms of various concentrations of As(III) in 0.1 M H_2SO_4 with the presence of a) 0.1 μM , b) 0.5 μM , and c) 5 μM As(V) in solution. d) Also shown are plots of the charge of peak 2' vs concentrations of As(III) in the absence and the presence of As(V) in 0.1 M H_2SO_4 at Au macroelectrodes. The concentrations of As(III) in voltammograms were 0.01 μM (black), 0.02 μM (red), 0.03 μM (blue), 0.05 μM (green), 0.07 μM (orange), and 0.1 μM (cyan). The charge was calculated from baseline corrected LSVs and the error bars shown are standard deviations calculated from at least three sets of data. The plots of charge vs concentrations of arsenic were As(III) (black), As(V) (red), As(III) in the presence of 0.1 μM As(V) (blue), As(III) in the presence of 0.5 μM As(V) (green), and As(III) in the presence of 5 μM As(V) (orange). ASV parameters: deposition at -0.9 V (for As(III)) or -1.3 V (for As(V)) vs. MSE for 300 s, potential scan rate 0.1 V s^{-1} , and baseline was modelled via the polynomial method from -0.1 V to $+0.22$ V for peak 2'. (For interpretation of the references to colour in this figure legend, the reader is referred to the Web version of this article.)

Table 1

The added concentrations of mixture of As(III)/As(V) and the measured total concentrations of arsenic and the As(V), As(III) concentrations. Measuring the total concentrations of arsenic used a deposition potential of -1.3 V and measuring the concentration of As(III) used a deposition potential of -0.9 V. The total concentrations of arsenic and the As(III) can be measured directly from the charge of peak 2', and the As(V) concentrations were obtained by subtraction of the As(III) concentration from the total arsenic concentration.

Added [As(III)+ As(V)] ($\mu\text{g L}^{-1}$)	Added [As(III)] ($\mu\text{g L}^{-1}$)	Added [As(V)] ($\mu\text{g L}^{-1}$)	Measured [As(III)+As (V)] ($\mu\text{g L}^{-1}$)	Measured [As(III)] ($\mu\text{g L}^{-1}$)	Measured [As(V)] ($\mu\text{g L}^{-1}$)
8.3	7.5	0.8	7.0	6.7 ± 2	0.3 ± 2
9.8	7.5	2.3	9.0	6.8 ± 2	2.2 ± 2
12	4	8	12	4 ± 2	8 ± 2
15	4	11	13	4 ± 2	9 ± 2
15	7.5	7.5	14	7.5 ± 2	6.5 ± 2
19	8	11	15	7.5 ± 2	7.5 ± 4
23	15	8	19	14 ± 4	5 ± 4
26	15	11	23	14 ± 4	9 ± 4

concentrations; the values are shown in Table 1 (Columns 3 and 6). The values are in reasonable agreement with the known values except at very low concentrations, below ca $3 \mu\text{g L}^{-1}$, where the accumulation of errors

leads to loss of accuracy. However the method is designed for use in drinking water samples where the total arsenic concentration is the key measurement; the relative amount of As (III) and As(V) as measured using UPD-ASV nevertheless give a clear indication of the speciation of As in the water.

Last gold screen printed electrodes (Au SPEs) were tested to see if they could replace gold macroelectrodes for As detection via the UPD-ASV method. However, the high capacitive currents and high background signal made it impossible to transfer this method onto the Au SPEs.

3.4. Interference study

Next an interference study was made for Cu(II) since it is a common interferent in the stripping voltammetry of bulk As since it can form Cu-As alloys during the deposition step [55]. The possible interference of Cu(II) with the detection of 0.1 μM As(V) was studied using UPD-ASV by adding different amounts of Cu(II). The pre-concentration was conducted at -1.3 V for 300 s, then followed with a linear potential scan from -1.3 V to $+0.6$ V at a scan rate of 0.1 V s^{-1} . Fig. 8a illustrates the raw voltammograms with the addition of different amount of Cu(II) from 1 μM to 1 mM at Au macroelectrodes. A peak observed at ca -0.3 V represented to the oxidation peak of Cu to Cu(II) [56] and increased with

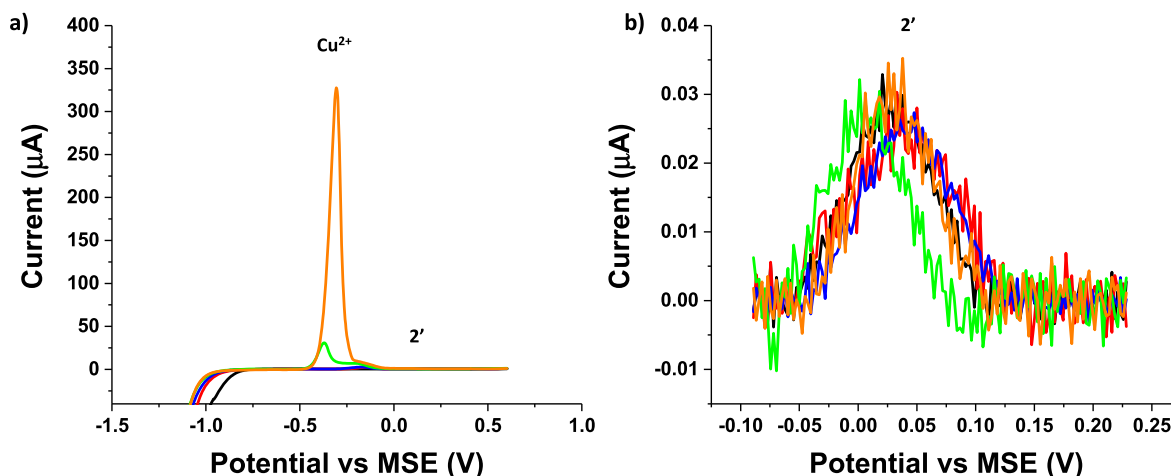


Fig. 8. a) Raw and b) baseline corrected ASV curves of 0.1 μM As(III) in 0.1 M H_2SO_4 with various concentrations of Cu^{2+} at Au macroelectrodes. Baseline corrected ASV curves of 0.1 μM As(III) in 0.1 M H_2SO_4 with various concentrations of Cu^{2+} in the potential range from -0.1 V to +0.23 V. ASV parameters: deposition at -1.3 V for 300 s, scan rate was 0.1 V s^{-1} . Cu(II) concentration: 0 μM (black), 1 μM (red), 10 μM (blue), 100 μM (green), and 1 mM (orange). (For interpretation of the references to colour in this figure legend, the reader is referred to the Web version of this article.)

the concentration of Cu(II) . The peak 2', corresponding to the oxidation of As ad-atoms was at $\text{ca} + 0.05 \text{ V}$. A baseline corrected voltammogram was made for peak 2' with the procedure above. Fig. 8b shows the baseline corrected stripping voltammograms of 0.1 μM As(V) with different amounts of Cu(II) from 1 μM to 1 mM at Au macroelectrodes. The black line was solution in the absence of Cu(II) and only peak 2' was observed at $\text{ca} + 0.05 \text{ V}$. With the addition of Cu(II) , the charge of peak 2' varied negligibly. Thus, it can be concluded that Cu(II) does not interfere to the oxidation peak of As ad-atoms on Au macroelectrodes even the deposition potential was at -1.3 V. We infer that the copper forms discrete deposits leaving almost all the Au surface free for As UPD.

4. Conclusions

The analytical use of underpotential deposition of As on gold surface with anodic stripping of adsorbed As ad-atoms on gold macroelectrodes has been shown to allow the detection of total As content by deposition at high potentials (-1.3 V vs MSE) and, selectively, of As(III) by deposition at lower potential (-0.9 V vs MSE). Limits of detections were found to be $0.8 \mu\text{g L}^{-1}$ (ppb) which are well within the WHO requirements for drinking water were observed for both As(III) and As(V) with visually discernible signals.

Credit author statement:

Yifei Zhang: Formal analysis, Investigation, Writing- Original draft. Prof. Dr. **Richard G. Compton:** Writing- Review & Editing, Supervision, Project administration

Declaration of competing interest

The authors declare that they have no known competing financial interests or personal relationships that could have appeared to influence the work reported in this paper.

Appendix A. Supplementary data

Supplementary data to this article can be found online at <https://doi.org/10.1016/j.talanta.2022.123578>.

References

- [1] J. Wang, *Stripping Analysis: Principles, Instrumentation, and Applications*, Vch Pub, 1985.

- [2] K. Brainina, E. Neyman, *Electroanalytical Stripping Methods*, John Wiley & Sons, 1994.
- [3] R.G. Compton, C.E. Banks, *Understanding Voltammetry*, third ed., World Scientific, 2018.
- [4] M. Fleischmann, S. Pons, The behavior of microelectrodes, *Anal. Chem.* 59 (1987) 1391A–1399A.
- [5] C. He, M. Tao, C. Zhang, Y. He, W. Xu, Y. Liu, W. Zhu, Microelectrode-based electrochemical sensing technology for in vivo detection of dopamine: recent developments and future prospects, *Crit. Rev. Anal. Chem.* (2020) 1–11.
- [6] R.G. Compton, G.G. Wildgoose, N.V. Rees, I. Streeter, R. Baron, Design, fabrication, characterisation and application of nanoelectrode arrays, *Chem. Phys. Lett.* 459 (2008) 1–17.
- [7] Y. Zhang, D. Li, R.G. Compton, Arsenic (III) Detection with Underpotential Deposition and Anodic Stripping Voltammetry, *ChemElectroChem*, 2021.
- [8] L.J. Bu, J. Liu, Q.J. Xie, S.Z. Yao, Anodic stripping voltammetric analysis of trace arsenic(III) enhanced by mild hydrogen-evolution at a bimetallic Au-Pt nanoparticle modified glassy carbon electrode, *Electrochem. Commun.* 59 (2015) 28–31.
- [9] Z. Guo, M. Yang, X.-J. Huang, Recent developments in electrochemical determination of arsenic, *Curr. Opin. Electrochem.* 3 (2017) 130–136.
- [10] Y. Zhang, D. Li, R.G. Compton, Arsenic (III) detection with underpotential deposition on gold, *J. Electroanal. Chem.* (2022) 116154.
- [11] J.H. Yoon, G. Muthuraman, J. Yang, Y.B. Shim, M.S. Won, Pt-nanoparticle incorporated carbon paste electrode for the determination of Cu (II) ion by anodic stripping voltammetry, *Electroanalysis* 19 (2007) 1160–1166.
- [12] J. Pizarro, E. Flores, V. Jimenez, T. Maldonado, C. Saitz, A. Vega, F. Godoy, R. Segura, Synthesis and characterization of the first cyrhetrenyl-appended calix [4] arene macrocycle and its application as an electrochemical sensor for the determination of Cu (II) in bivalve mollusks using square wave anodic stripping voltammetry, *Sens. Actuators, B* 281 (2019) 115–122.
- [13] Z. Zhai, N. Huang, H. Zhuang, L. Liu, B. Yang, C. Wang, Z. Gai, F. Guo, Z. Li, X. Jiang, A diamond/graphite nanoplatelets electrode for anodic stripping voltammetric trace determination of Zn (II), Cd (II), Pb (II) and Cu (II), *Appl. Surf. Sci.* 457 (2018) 1192–1201.
- [14] A. Nsabimana, S.A. Kite, T.H. Fereja, M.I. Halawa, W. Zhang, G. Xu, Recent developments in stripping analysis of trace metals, *Curr. Opin. Electrochem.* 17 (2019) 65–71.
- [15] M. Dali, K. Zinoubi, A. Chrouda, S. Abderrahmane, S. Cherrad, N. Jaffrezic-Renault, A biosensor based on fungal soil biomass for electrochemical detection of lead (II) and cadmium (II) by differential pulse anodic stripping voltammetry, *J. Electroanal. Chem.* 813 (2018) 9–19.
- [16] H. Xiao, W. Wang, S. Pi, Y. Cheng, Q. Xie, Anodic stripping voltammetry analysis of mercury (II) on a pyridine-Au/pyridine/glassy carbon electrode, *Sens. Actuators, B* 317 (2020) 128202.
- [17] H. Abdolmohammad-Zadeh, R. Mohammad-Rezaei, A. Salimi, Preconcentration of mercury (II) using a magnetite@ carbon/dithizone nanocomposite, and its quantification by anodic stripping voltammetry, *Microchim. Acta* 187 (2020) 1–8.
- [18] Y. Xia, J. Li, G. Zhu, Y. Yi, Innovative strategy based on novel Ti3C2Tx MXenes nanoribbons/carbon nanotubes hybrids for anodic stripping voltammetry sensing of mercury ion, *Sens. Actuators, B* 355 (2022) 131247.
- [19] C.A. Paddon, R.G. Compton, Underpotential deposition of lithium on platinum single crystal electrodes in tetrahydrofuran, *J. Phys. Chem. C* 111 (2007) 9016–9018.
- [20] O.A. Oviedo, L. Reinaudi, S.G. García, E.P.M. Leiva, Underpotential Deposition, *Monographs in Electrochemistry*, 2016.

- [21] F.J. Sarabia, V. Climent, J.M. Feliu, Underpotential deposition of Nickel on platinum single crystal electrodes, *J. Electroanal. Chem.* 819 (2018) 391–400.
- [22] M.K. Yadav, D. Saidulu, A.K. Gupta, P.S. Ghosal, A. Mukherjee, Status and management of arsenic pollution in groundwater: a comprehensive appraisal of recent global scenario, human health impacts, sustainable field-scale treatment technologies, *J. Environ. Chem. Eng.* 9 (2021) 105203.
- [23] D. Banik, S.K. Manna, A.K. Mahapatra, Recent development of chromogenic and fluorogenic chemosensors for the detection of arsenic species: environmental and biological applications, *Spectrochim. Acta, Part A* 246 (2021) 119047.
- [24] M. Kobyra, R.D.C. Soltani, P.I. Omwene, A. Khataee, A review on decontamination of arsenic-contained water by electrocoagulation: reactor configurations and operating cost along with removal mechanisms, *Environ. Technol. Innovat.* 17 (2020) 100519.
- [25] D.Q. Hung, O. Nekrasova, R.G. Compton, Analytical methods for inorganic arsenic in water: a review, *Talanta* 64 (2004) 269–277.
- [26] N.R. Council, Chemistry and analysis of arsenic species in water, food, urine, blood, hair, and nails, in: *Arsenic in Drinking Water*, National Academies Press (US), 1999.
- [27] X.P. Yu, C.L. Liu, Y.F. Guo, T.L. Deng, Speciation analysis of trace arsenic, mercury, selenium and antimony in environmental and biological samples based on hyphenated techniques, *Molecules* 24 (2019) 23.
- [28] S. Li, C.C. Zhang, S.N. Wang, Q. Liu, H.H. Feng, X. Ma, J.H. Guo, Electrochemical microfluidics techniques for heavy metal ion detection, *Analyst* 143 (2018) 4230–4246.
- [29] S. Sikdar, M. Kundu, A review on detection and abatement of heavy metals, *ChemBioEng Rev* 5 (2018) 18–29.
- [30] X.C. Le, X. Lu, M. Ma, W.R. Cullen, H.V. Aposhian, B. Zheng, Speciation of key arsenic metabolic intermediates in human urine, *Anal. Chem.* 72 (2000) 5172–5177.
- [31] Who, Guidelines for drinking-water quality, *WHO Chron.* 38 (2011) 104–108.
- [32] J.A. Cox, I.A. Rutkowska, P.J. Kulesza, Critical review-electrocatalytic sensors for arsenic oxo species, *J. Electrochem. Soc.* 167 (2020) 6.
- [33] J. Lalmalsawmi, D. Tiwari, D.J. Kim, Role of nanocomposite materials in the development of electrochemical sensors for arsenic: past, present and future, *J. Electroanal. Chem.* 877 (2020) 18.
- [34] G.M. dos Santos, D. Pozebon, C. Cerveira, D.P. de Moraes, Inorganic arsenic speciation in rice products using selective hydride generation and atomic absorption spectrometry (AAS), *Microchem. J.* 133 (2017) 265–271.
- [35] I. Komorowicz, A. Hanć, W. Lorenc, D. Barańkiewicz, J. Falandysz, Y. Wang, Arsenic speciation in mushrooms using dimensional chromatography coupled to ICP-MS detector, *Chemosphere* 233 (2019) 223–233.
- [36] H. Cheng, W. Zhang, Y. Wang, J. Liu, Graphene oxide as a stationary phase for speciation of inorganic and organic species of mercury, arsenic and selenium using HPLC with ICP-MS detection, *Microchim. Acta* 185 (2018) 1–8.
- [37] A.K. Sakira, I.T. Somé, E. Ziemons, B. Dejaegher, D. Mertens, P. Hubert, J. M. Kauffmann, Determination of arsenic (III) at a nanogold modified solid carbon paste electrode, *Electroanalysis* 27 (2015) 309–316.
- [38] I. Švancara, K. Vytrás, A. Bobrowski, K. Kalcher, Determination of arsenic at a gold-plated carbon paste electrode using constant current stripping analysis, *Talanta* 58 (2002) 45–55.
- [39] W.B. Postek, I.A. Rutkowska, J.A. Cox, P.J. Kulesza, Electrocatalytic effects during redox reactions of arsenic at platinum nanoparticles in acid medium: possibility of preconcentration, electroactive film formation, and detection of as (III) and as (V), *Electrochim. Acta* 319 (2019) 499–510.
- [40] E.A. Zakharova, G.N. Noskova, S.G. Antonova, A.S. Kabakaev, Speciation of arsenic (III) and arsenic (V) by manganese-mediated stripping voltammetry at gold microelectrode ensemble in neutral and basic medium, *Int. J. Environ. Anal. Chem.* 94 (2014) 1478–1498.
- [41] C.M.A. Brett, A.M.O. Brett, *Electroanalysis*, Oxford Science Publications, 1998.
- [42] H. Huang, P.K. Dasgupta, A field-deployable instrument for the measurement and speciation of arsenic in potable water, *Anal. Chim. Acta* 380 (1999) 27–37.
- [43] D. Yamada, T.A. Ivandini, M. Komatsu, A. Fujishima, Y. Einaga, Anodic stripping voltammetry of inorganic species of As³⁺ and As⁵⁺ at gold-modified boron doped diamond electrodes, *J. Electroanal. Chem.* 615 (2008) 145–153.
- [44] L. Xiao, G.G. Wildgoose, R.G. Compton, Sensitive electrochemical detection of arsenic (III) using gold nanoparticle modified carbon nanotubes via anodic stripping voltammetry, *Anal. Chim. Acta* 620 (2008) 44–49.
- [45] M. Baghayeri, M. Ghanei-Motlagh, R. Tayebie, M. Fayazi, F. Narenji, Application of graphene/zinc-based metal-organic framework nanocomposite for electrochemical sensing of as (III) in water resources, *Anal. Chim. Acta* 1099 (2020) 60–67.
- [46] M. Nodehi, M. Baghayeri, H. Veisi, Preparation of GO/Fe₃O₄@ PMDA/AuNPs nanocomposite for simultaneous determination of As³⁺ and Cu²⁺ by stripping voltammetry, *Talanta* 230 (2021) 122288.
- [47] M. Baghayeri, A. Amiri, F. Karimabadi, S. Di Masi, B. Maleki, F. Adibian, A. R. Pourali, C. Malitesta, Magnetic MWCNTs-dendrimer: a potential modifier for electrochemical evaluation of as (III) ions in real water samples, *J. Electroanal. Chem.* 888 (2021) 115059.
- [48] A.J. Bard, L.R. Faulkner, *Electrochemical Methods: Fundamentals and Applications*, second ed., John Wiley & Sons, Inc, New York, 2001.
- [49] Zimmer&Peacock, *Cleaning Gold Electrodes*, 2017.
- [50] J. Zheng, W. Goessler, W. Kosmus, The chromatographic behavior of arsenic compounds on anion exchange columns with binary organic acids as mobile phases, *Chromatographia* 47 (1998) 257–263.
- [51] L. Bu, T. Gu, Y. Ma, C. Chen, Y. Tan, Q. Xie, S. Yao, Enhanced cathodic preconcentration of as (0) at Au and Pt electrodes for anodic stripping voltammetry analysis of as (III) and as (V), *J. Phys. Chem. C* 119 (2015) 11400–11409.
- [52] X. Dai, O. Nekrasova, M.E. Hyde, R.G. Compton, Anodic stripping voltammetry of arsenic (III) using gold nanoparticle-modified electrodes, *Anal. Chem.* 76 (2004) 5924–5929.
- [53] A. Buffa, D. Mandler, Arsenic (III) detection in water by flow-through carbon nanotube membrane decorated by gold nanoparticles, *Electrochim. Acta* 318 (2019) 496–503.
- [54] D. Wang, Y. Zhao, H. Jin, J. Zhuang, W. Zhang, S. Wang, J. Wang, Synthesis of Au-decorated tripod-shaped Te hybrids for applications in the ultrasensitive detection of arsenic, *ACS Appl. Mater. Interfaces* 5 (2013) 5733–5740.
- [55] A. Jimana, M.G. Peleyeju, L. Tshwenya, K. Pillay, O.A. Arotiba, Voltammetric analysis of as(III) at a cobalt nanoparticles/reduced graphene oxide modified exfoliated graphite electrode, *Int. J. Electrochem. Sci.* 13 (2018) 10127–10140.
- [56] C. Gao, X.-Y. Yu, S.-Q. Xiong, J.-H. Liu, X.-J. Huang, Electrochemical detection of arsenic (III) completely free from noble metal: Fe₃O₄ microspheres-room temperature ionic liquid composite showing better performance than gold, *Anal. Chem.* 85 (2013) 2673–2680.